Hindawi
Geofluids
Volume 2021, Article ID 8875249, 17 pages
https://doi.org/10.1155/2021/8875249

Research Article

Disaster Control of Roof Falling in Deep Coal Mine Roadway Subjected to High Abutment Pressure

Shizhong Zhang,[1,2] **Gangwei Fan**,[1,2] **Ling Chai**,[2] **Qizhen Li**,[2] **Mingwei Chen**,[3] **Tao Luo**,[2] **and Shang Ren**[2]

[1]*State Key Laboratory of Coal Resources and Safe Mining, China University of Mining & Technology, No. 1 University Road, Xuzhou, Jiangsu 221116, China*
[2]*School of Mines, China University of Mining & Technology, No. 1 University Road, Xuzhou, Jiangsu 221116, China*
[3]*School of Minerals and Energy Resources Engineering, The University of New South Wales, Sydney 2052, Australia*

Correspondence should be addressed to Gangwei Fan; fangw@cumt.edu.cn

Received 15 May 2020; Revised 25 September 2020; Accepted 23 December 2020; Published 12 January 2021

Academic Editor: Andrea Brogi

The roof falling accident is a serious threat to the lives of miners in deep coal mining, especially when the coal mine is more than 1000 meters deep. In regard to the 5306 coalface in the Tangkou coal mine, Shandong, China, the depth of coal seam is 992.8 m and the stress concentration coefficient of the roadway surrounding rock is 3.33. This leads to a serious deformation of the roadway roof, thereby producing a high risk of the roof falling disaster. In this pursuit, based on the mechanical analysis of roadway roof subjected to a high abutment pressure, the mathematical expressions of the setting load and movable column length of supports were introduced. Furthermore, the stability control mechanism of the roadway roof was analyzed and the optimized support parameters of supports are provided. The results showed that the longtime effective support of the roadway roof required the strength and deformation coupling of supports and anchored surrounding rock. The support length of the belt roadway should be at least 57.7 m, with 0-30 m away from the coalface supported by hydraulic supports and 32-57.7 m supported by single props. In addition, the maximum setting load and movable column length of hydraulic supports were 21.67 MPa and 280.3 mm and 12.44 MPa and 177.1 mm for single props, respectively. By applying the optimized support parameters of supports to the belt roadway of the 5306 coalface, the effective control of the roadway roof and the disaster control of roof falling were realized.

1. Introduction

Roof falling accident has always been one of the major mine disasters that pose threats to the life of the underground miners in coal mining [1]. Statistical data associated with coal mine accidents in China shows that roof falling accidents occurred most frequently in all kinds of mine accidents. The number of roof falling accidents was 760, and the accident concerning roof falling accounted for 39% of the total cases between 2013 and 2017, while the accident concerning roof falling accounted for 34% the of total cases in 2018 [2]. Among them, the roof falling arising in the roadway of the intersection area of coalface and roadway was the most common. For example, on January 17, 2017, a roof falling accident took place in the transportation roadway subjected to front abutment pressure of 2403 coalface of the Danshuigou coal mine in Shanxi Province, China, resulting in the death of 10 people; on November 11, 2017, a similar accident occurred in the ventilation roadway subjected to the front abutment pressure of the 702 coalface of Hongyangsan coal mine in Liaoning Province, China, resulting in 10 deaths. A similar accident arising in Longgu coal mine in Shandong Province also led to 4 deaths on February 22, 2020. These cases demonstrate the terrible impacts of the roof falling accident on the production of coal mine and the safety of miners.

The roof falling accidents occur in the intersection area of the coalface and the roadway due to the stress redistribution in the surrounding rock, thereby generating an abutment pressure in front of the coalface [3]. Such abutment pressure moves forward dynamically with the coalface retreat and correspondingly facilitates a stress-concentrated area above the roadway (Figure 1(a)). Especially, the stress concentration

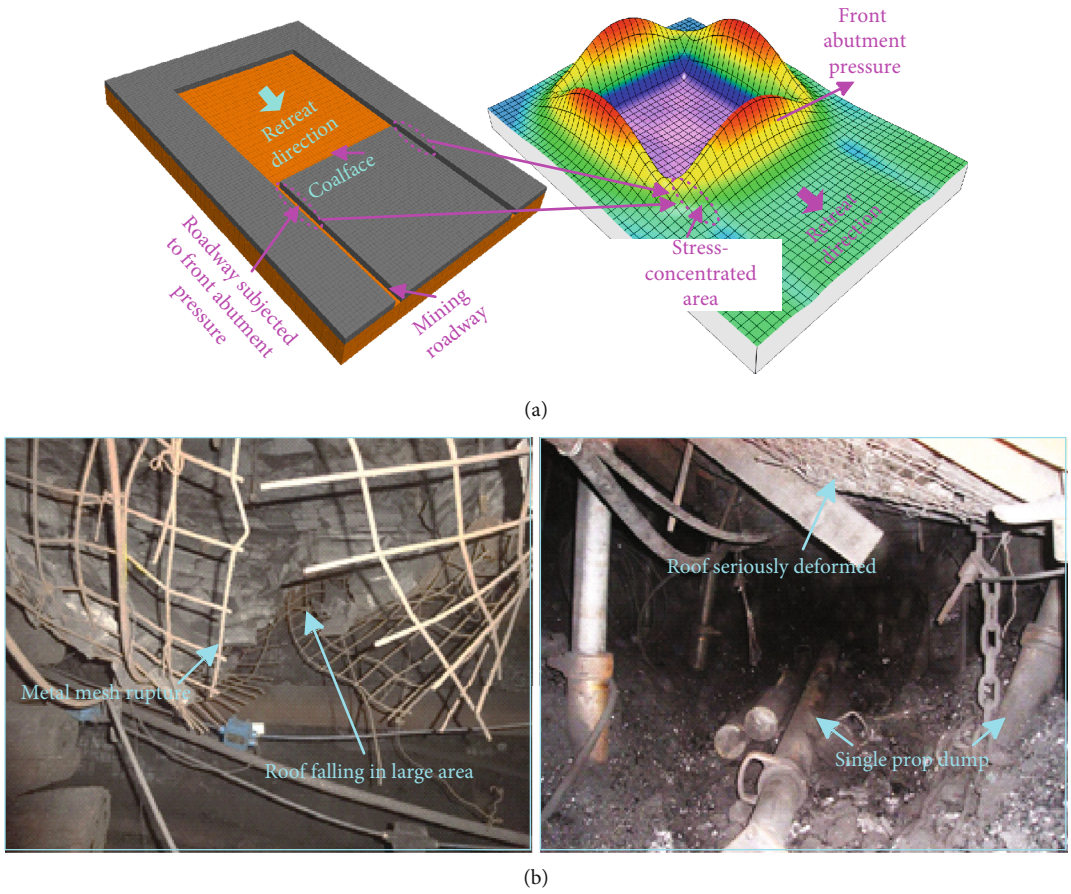

Figure 1: Stress distribution and roof falling disaster in the roadway subjected to the dynamic abutment pressure: (a) stress distribution characteristics; (b) roof falling disaster.

coefficient of the overburden is 3-8 times of the primary rock stress, when the coalface is more than 1000 m deep. The high concentrated stress (also called the front abutment pressure) causes the overlying strata to experience the loading and unloading process repeatedly. As a result, it is relatively difficult for the surrounding rock of this area to be controlled under the influence of high concentrated stress, leading to hazards like mesh fracture, large-scale roof falling, and supporting equipment collapse (shown in Figure 1(b)) that pose a serious threat to the miners' safety [4, 5]. When underground coal mining is carried out deeper than 1000 m, with the sharp increase in the ground stress, the burst tendency of coalface is higher, and the peak and range of the abutment pressure before the coalface are higher. This makes it more difficult to restrain the surrounding rocks; thus, the roof falling hazards become an important issue challenging the safety production of coal mines. Currently, the roof control of the roadway subjected to an abutment pressure with the depth more than 1000 m is mainly implemented by the means of temporary reinforced supporting using single props or hydraulic supports. However, the computation in terms of the supporting parameters is mainly based on the accumulated experience and lacks theoretical foundation. Also, the interaction between the supports and the surrounding rocks is not explicit, and the corresponding mechanism of stability control of surrounding rocks remains unclear. These points trigger the frequent occurrence of roof falling accidents of the roadway subjected to an abutment pressure and increase the exposure of hazards to the miners.

Different from that in other locations, the roof control of the roadway subjected to a front abutment pressure is achieved through the coupling of supports (such as hydraulic supports or single props) and anchored surrounding rock (bolt-mesh-anchor support). During mining in the coalface, the hydraulic supports or single props are typically employed to support the roadway, which are subjected to front abutment pressure for reinforcement and ensure sufficient cross-area for mining. Prior to the installment of the supports, the anchored surrounding rock in the roadway already has a certain bearing capacity due to the support provided by the existing bolt-mesh-anchor support. Without enough supporting capacity of the supports, it is unlikely to effectively control the deformation and failure of the surrounding rock despite the existing bearing capacity of the bolt-mesh-anchor support. In contrast, the excessive supporting capacity of the supports can disturb the existing bolt-mesh-anchor support system, resulting in an insufficient development of the bearing capacity of the surrounding rock. This proves that the supports and the anchored surrounding rock in the roadway subjected to the front abutment pressure are mutually related and influence each other, and a coupling relationship exists between them. When the coupled support of the

supports and the anchored surrounding rock is achieved, the bearing capacities of both can fully control the deformation of the surrounding rock in the roadway subjected to a front abutment pressure. Therefore, the study of the relation between supports and anchored surrounding rock subjected to front abutment pressure and the effective control of roadway roof in the coalface are of great significance to reduce the roof falling disaster and ensure the safety of the miners in coal mines.

Currently, a few studies have been conducted on the relation between the supports and the anchored surrounding rock subjected to front abutment pressure. Wang and Niu introduced the strength coupling between the support system and surrounding rock subjected to front abutment pressure and the notions of structural and stability coupling, but their application in mines was limited [6]. Some studies were mainly focused on the interaction between the hydraulic supports and the surrounding rock in the coalface [7–9]. For example, Mangal and Paul and Ma and Zhong found that the load of the hydraulic supports in the coalface depended on the mining height, thickness of the immediate roof, plastic zone range in the coal wall, and the mechanical strength of the roof and floor [10, 11]. Yuan et al. and Peng proposed that the study of the interaction between the hydraulic supports and the surrounding rock in the coalface should consider the coal wall, roof, floor and supports, and regard them as a unit [12, 13]. It is reported that the setting load and work resistance of the hydraulic supports were crucial to maintain the stability of the system [14, 15]. Based on the long-term field monitoring and theoretical analyses, Budirský proposed a method for determining the setting loading and working resistance of the hydraulic supports in the rock burst coalface [16]. Singh and Singh proposed that the notion of "the bigger, the better" was not fully scientific, while choosing the hydraulic supports in the coalface and controlling the deformation of roadway roof, and stated that the setting load of the hydraulic supports in coal mines was usually 50–60% of the work resistance in Indian mines [17, 18]. Xu and Liu found that the setting load of hydraulic supports in the coalface directly impacted the support stiffness. A small setting load caused a large settlement of the roof, resulting in the falling of the roof [19]. Even though these studies clarified the interaction between the hydraulic supports and the surrounding rock in the coalface, the supports in the roadway subjected to front abutment pressure present some features that are different from the coalface. Hydraulic supports in the coalface can bear the additional pressure caused by the weight of the immediate roof rocks and main roof pressure. As a result, the supports need a certain capacity to bear the impact load in order to prevent the rock blocks rolling into the coalface and goaf from the roof and causing harm to the equipment and miners. Supports in the roadway subjected to the front abutment pressure are to bear the high stresses above the roadway roof caused by the front abutment pressures (Figure 1(a)) in order to ensure sufficient section. Due to the differences in using location, stress environments, bearing capacities, and effects of the roof control between the hydraulic supports in the coalface and the roadway subjected to a front abutment pressure, the results of the previous studies on hydraulic supports in coalface are not applicable to describe the coupling of supports and anchored surrounding rock in the roadway. However, previous analysis methods and conceptions still provide guidance for the present study.

With respect to elucidating the relations between the supports and the anchored surrounding rock, the first problem that needs to be solved is the stability of the roadway roof subjected to the front abutment pressure. Studies on the stability of the roadway roof mainly focused on the location unaffected by the front abutment pressure, which resulted in many achievements [20–23]. For instance, Sofianos regarded the roadway roof as a hinged roof beam on a rigid foundation and introduced three deformation forms in the hard rock: rotation failure, sliding failure, and squeezing failure [24]. Chase et al. found that under high vertical stresses, the vertical splitting fractures developed in the direction of cleating, thereby causing a scaling of the roadway [25]. Canbulat and Tadolini et al. found that the deformation forms of the roadway roof consisted the shear failure and bucking failure, and proposed the corresponding control methods [26, 27]. Based on previous studies, Shen summarized the failure patterns of the surrounding rock in the soft rock roadway as six types, including beam failure, joint-controlled rock falls, and roof sag [28]. Kang et al. and Carranza-Torres found that the bolt-cable support in the surrounding rock effectively reduced the contraction rate of the roadway and restrained or eliminated the tension failure [29, 30]. Due to the special conditions of the surrounding rock in the roadway subjected to the front abutment pressure, studies of the roadway roof stability should consider the supporting effect of the hydraulic supports and the bolt-mesh-anchor support on the roof, which has not been thoroughly considered by previous researchers.

In the present study, the support in the belt roadway subjected to the front abutment pressure of the 5306 coalface of the Tangkou coal mine in Shandong Province, China, was selected as a case study. Firstly, the mechanisms of the roadway deformation and failure subjected to abutment pressure in the 5306 coalface (with a depth of 1000 meters) were analyzed. Subsequently, the stability of the roadway roof with the hydraulic supports and the bolt-mesh-anchor support, as well as the method for determining the related support parameters (including support strength and movable column length of supports), was analyzed. Finally, the relation between the supports and the anchored surrounding rock, as well as the stability control mechanism of roadway roof, was clarified. Based on these, the support parameters were optimized to ensure the safety of the miners and for a sustainable mining in the Tangkou coal mine.

2. Study Site

2.1. Geological Setting. The depth and coal thickness of the 5306 coalface in the Tangkou coal mine were 992.8 m and 5 m, respectively, with an average angle of inclination of 4°. In addition, two faults were detected in the 5306 coalface, and the maximum drop was 3.0 m and 2.7 m, respectively, which had a little impact on the coal mining of coalface. The coal seam in the 5306 coalface was stable, and there

was no erosion zone and collapse column. There were only some small undulating folds in the mining area, which did not affect the retreat of the coalface. The comprehensive geological column of the 5306 coalface is shown in Figure 2.

2.2. Layout and Support of the Roadway. The 5306 coalface was divided into inner and outer segments: the inner segment was 248 m wide and had a strike mining length of 1000 m; the outer segment was 795 m wide and had a strike mining length of 1065 m. The track roadway was in close proximity to the goaf of the 5305 coalface. The belt roadway of the coalface had a rectangular cross section with a width of 5000 mm and a height of 4000 mm, with entity coals on two sides. The roadway layout of 5306 coalface is shown in Figure 3(a). Hydraulic supports and single props were used as the supporting methods in the roadway subjected to front abutment pressure. The support length was 60 m. Three groups of hydraulic supports (ZQL2×2500/23/42W) were used in the roadway; the length of each group was 10.4 m, with a support range of 0–31.2 m in front of the coalface. A total of 36 rows of single props (DW45-250/110XL(G)) were used, with 2 props placed in each row, coupled with an articulated roof beam (DJB-800). The support pattern was "one beam for one prop,", with a support range of 32–60 m in front of the coalface. The hydraulic supports had a setting load of 6.5 MPa and a movable column length of 350 mm, and the single props had a setting load of 11.5 MPa and a movable column length of 100 mm.

The field practice shows that deformation and failure of the surrounding rock in the roadway subjected to the front abutment pressure were serious with the original support pattern employed in the coalface. The rocks in the roof crushed with a large settlement, forming a "net trough"; the rocks within the net trough fractured and fell when the deformation was large, risking the safety of the miners and the equipment (as shown in Figures 3(b) and 3(c)). Additionally, the entity coal sides showed a large deformation and extrusion to the roadway centerline, presenting an arc shape and significantly reducing the available cross section. In practice, the bottom mining and expansion are typically applied in the roadway to obtain sufficient available cross section and ventilation, which actually disturb the mining in the coalface.

3. Failure Mechanisms

To analyze the deformation and failure mechanism of the surrounding rock in the roadway subjected to front abutment pressure, a 3DEC numerical modeling was constructed with the same support parameters as in the field.

3.1. Model Construction. The physical and mechanical parameters of the rock stratum in the numerical model are shown in Table 1. The bolt material was a 20 MnSi screw thread steel bolt without longitudinal reinforcement with a diameter of 20 mm. The cable material was 1 × 19 core low relaxation prestressed steel strand anchor cable with a diameter of 21.8 mm. The lengths of the bolt used in roadway roof and two sides were 2400 mm and 3000 mm, respectively. The length of the cable was 6200 mm. To support the roadway

COLUMN	LITHOLOGY	THICKNESS	REMARK
	Mudstone	7.7 m	
	Fine sandstone	8.0 m	
	Mudstone	7.3 m	
	Siltstone	7.5 m	
	Fine sandstone	5.4 m	Main roof
	Mudstone	2.5 m	Immediate roof
	3# Coal seam	5.0 m	Roadway
	Mudstone	6.0 m	Floor
	Siltstone	6.1 m	

Figure 2: Comprehensive geological column of the 5306 coalface.

roof with a row and line space of 900 × 1200 mm, 6 bolts and 5 cables were used. To support the roadway side with a row and line space of 900 × 800 mm, 5 bolts were employed. Furthermore, the size of the numerical model was 400 m × 300 m × 56 m (length × width × height). The four sides and the bottom of the model were fixed constraints to limit the displacement. A uniform load of 23.85 MPa was applied vertically to the upper surface of the model according to the in situ stress condition of the 5306 coalface. In the numerical simulation, the Mohr-Coulomb model was used for iterative solution. The numerical model established is shown in Figure 4.

3.2. Modelling Results. Based on the numerical model, the vertical displacement and vertical stress of the roadway at 20 m and 30 m in front of the coalface are shown in Figures 5 and 6.

Using the same parameters as those in the roadway support in the field, the surrounding rock in the roadway at 20 m in front of the coalface showed a large deformation (Figure 5). The roadway roof significantly settled, forming a net trough with a maximum settlement of 659.9 mm; a roof separation was also observed, with both sides of the roadway extruding and forming an arc shape. These features were similar to those recorded in the field (Figure 5(a)). Additionally, some bolts in the coal sides and roof became dislocated and lost their bearing capacity. The side abutment pressures in the coal sides were symmetrical, and a stress-concentrated core area was formed with an ear shape, where the maximum vertical stress was 82.58 MPa and the stress concentration coefficient was 3.33. The deformation pattern of the surrounding rock in the roadway at 35 m in front of the coalface was almost the same as that at 20 m (Figure 6). The difference was that the maximum settlement of the roadway roof was 407.0 mm and the maximum vertical stress was 54.11 MPa of the surrounding rock in the roadway at 35 m in front of the coalface; both were smaller than their counterparts in the roadway at 20 m in front of the coalface. Moreover, there was a stress-concentrated area with a small range in the place where the immediate roof and support met.

Based on the numerical simulations and original support effect on-site, it was predicted that the surrounding rock in the roadway at 20 m in front of the coalface presented a

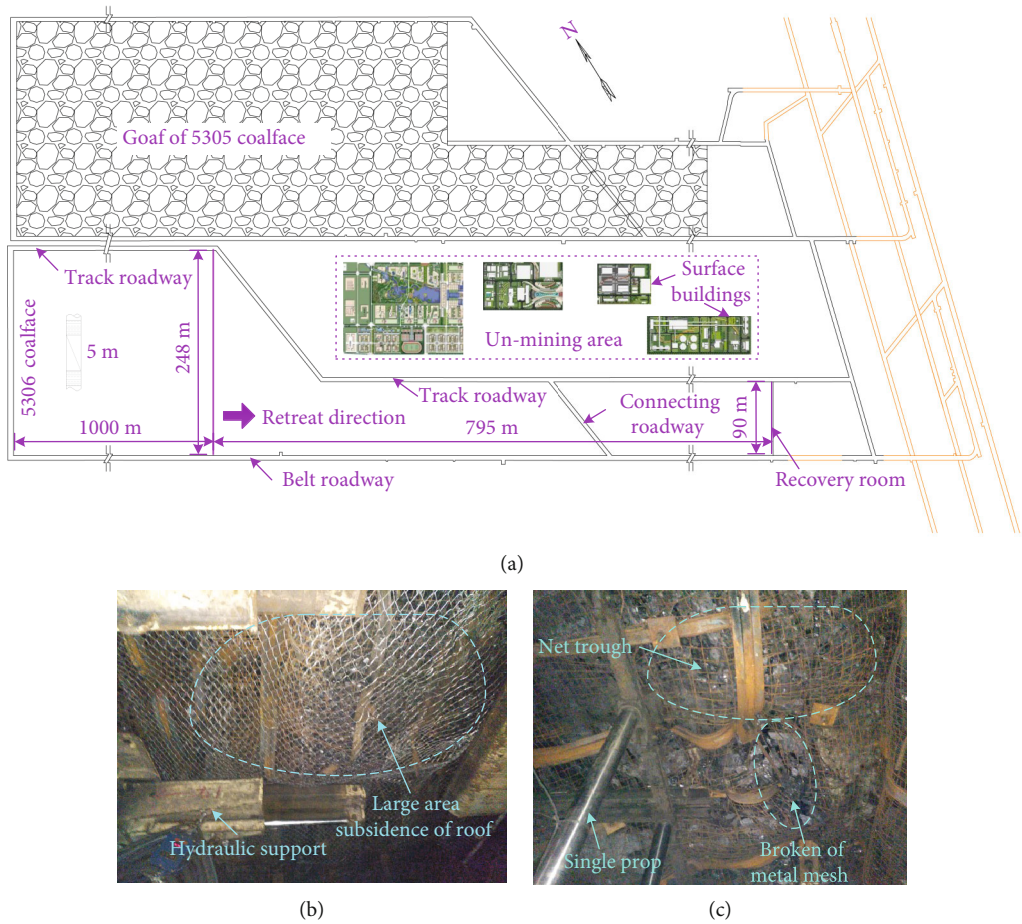

Figure 3: Layout and failure characteristics of roadway: (a) the roadway layout of the 5306 coalface; (b) area of 20 m in front of the workface; (c) area of 35 m in front of the workface.

Table 1: Physical and mechanical parameters of rock stratum.

Lithology	Density (kg/m^3)	Bulk modulus (GPa)	Shear modulus (GPa)	Internal friction angle (°)	Cohesive force (MPa)	Tensile strength (MPa)	Remark
Mudstone	2540	2.35	1.52	32	1.7	1.57	
Fine sandstone	2831	3.22	1.80	35	2.3	2.24	
Mudstone	2450	1.25	1.66	37	2.1	1.60	
Siltstone	2635	2.16	1.23	39	3.3	1.80	
Fine sandstone	2632	4.12	2.30	33	3.3	2.89	Main roof
Mudstone	2643	0.96	0.93	30	1.5	0.87	Immediate roof
3# coal seam	1401	0.68	0.50	26	0.9	0.41	
Mudstone	2651	2.55	1.52	42	2.6	2.00	Floor
Siltstone	2645	2.57	1.54	34	2.5	2.68	

substantial dislocation deformation, with some bolts not functioning and separating in the roof. This was likely, due to the failure of providing enough support strength caused by an insufficient setting load or the excessively large prop movable column in the hydraulic support (the setting load and movable column length of hydraulic supports were 6.5 MPa and 300 mm, respectively, in the field). The deformation and failure of the surrounding rock in the roadway at 35 m in front of the coalface and the increase in stress in the roof surface could be due to the failure of timely yielding

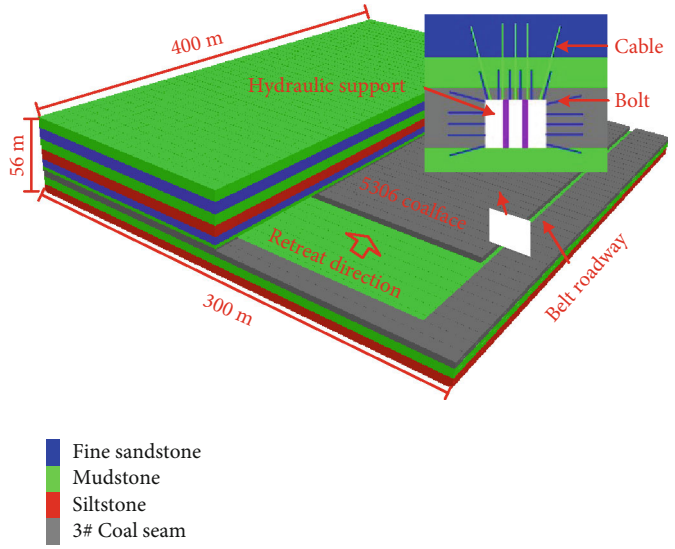

Figure 4: Establishment of the numerical model.

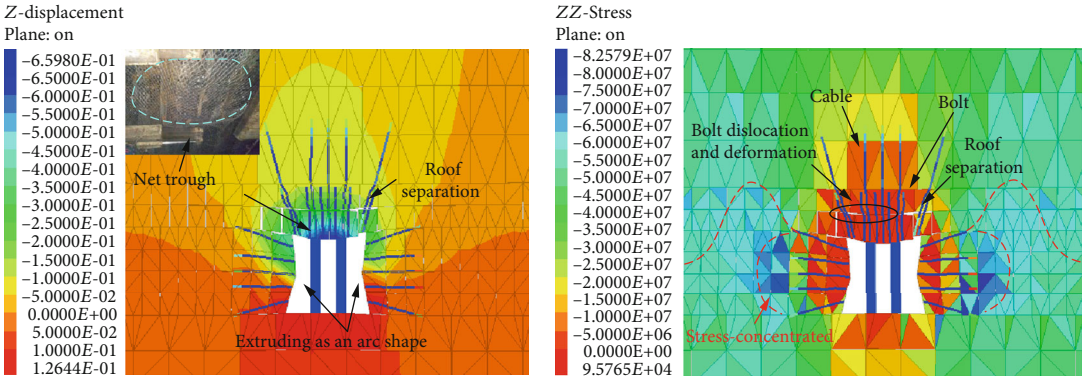

Figure 5: Numerical simulation results of the surrounding rock deformation at 20 m in front of the coalface: (a) cloud graph of vertical displacement; (b) cloud graph of vertical stress.

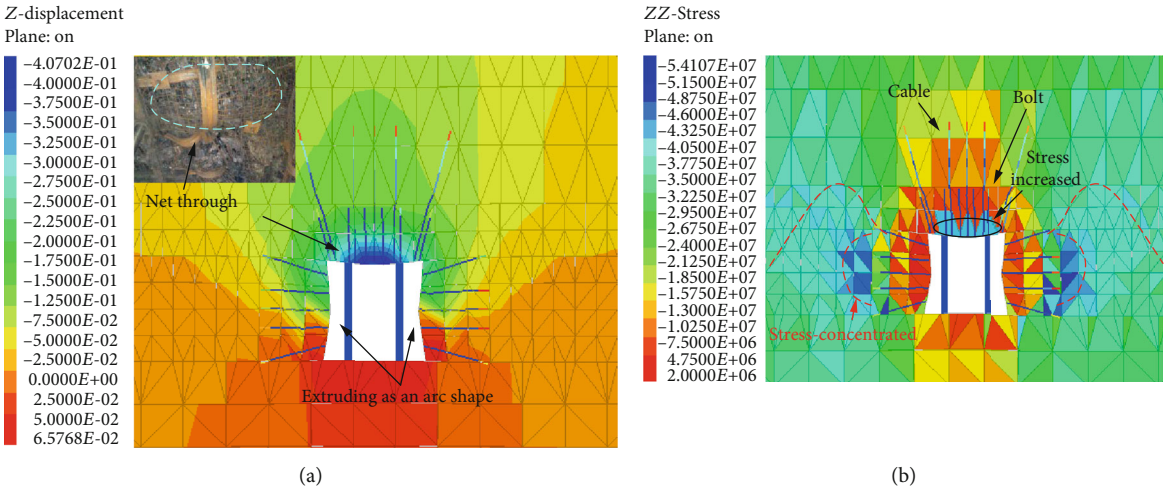

Figure 6: Numerical simulation results of the surrounding rock deformation at 35 m in front of the coalface: (a) cloud graph of vertical displacement; (b) cloud graph of vertical stress.

caused by the excessively small prop movable column (the movable column of the single props was 100 mm in the field). These characteristics showed that the deformation of the surrounding rock in the roadway subjected to front abutment pressure of the coalface was closely related to the support strength and movable column length of supports.

4. Stability Control of Roadway Roof

4.1. Mechanical Analysis

4.1.1. Construction of the Mechanical Model. The coal sides were regarded as the Winkler foundation, since the entity coal sides were weak, while the roadway roof was regarded as a semi-infinite elastic cantilever beam based on the Winkler foundation, with the stress increments of the overlaying rock acting on it. The perspective of the mechanical model was perpendicular to the layout direction of belt roadway. Considering the symmetry of the roadway and the support to the roof, the mechanical model of the roadway roof subjected to the front abutment pressure was established, as shown in Figure 7. It should be noted that the plastic zone in the surrounding rock of roadway was not considered in the mechanical model.

To facilitate the theoretical analysis of the roadway roof deformation, a deformable foundation with a constant load and a constant rigidity was used as an equivalent for analysis of the fractures and stress reduction in the coal sides, which also had a good fit with the practice in the field [31]. The vertical stress increment caused by the mining and the support forces of the hydraulic support were considered, but the overall deformation of the model caused by γH was not taken into consideration. In the model, q_z is the upper load from the roof, which is regarded as a uniform load; $q(x)$ is the side abutment pressure from the coal sides, with a peak value q_1 in the boundary, that is, $x = 0$, and is zero at $x = x_1$; q_a is the support strength to keep the surrounding rock stable, which is also regarded as a uniform load; B is the width of the roadway; Q_0 and M_0 are the shear force and bending moment on the elastic foundation boundary, respectively; and M_z is the bending moment on the left side of the model (as shown in Figure 7).

4.1.2. Mechanical Derivation. Based on the above model, Jiang et al. deduced the bending moment $M_r(x)$ and deflection $y_r(x)$ of the roadway roof in detail when the support strength q_a was not considered and x was in the range $-B/2 \le x \le 0$ [31]. Details of the equations are not included here, and these two parameters are given in Equations (1) and (2):

$$M_r(x) = \varphi_0 \frac{q_z B^2}{12} + q_z B x + \frac{q_z x^2}{2}, \tag{1}$$

$$y_r(x) = \frac{1}{EI}\left\{-\varphi_z \frac{q_z B^2}{48} x^2 + \frac{q_z}{24}\left[\frac{B}{2} + x\right]^4 - \varphi_z \frac{q_z B^2}{48} B x \cdot + \frac{EI}{k}\left[q_z \lambda B + \varphi_0 \frac{q_z \lambda^2 B^2}{6}\right] + \frac{q_1}{\lambda x_1}[\lambda x_1 - \xi(x_1)] - \frac{q_z}{24}\left[\frac{B}{2}\right]^4\right\}, \tag{2}$$

where λ is the characteristic factor, and $\lambda = \sqrt[4]{k/4EI}$; φ_0, φ_z are the modification factors of the bending moment of the abutment and the middle point of the roof; and $\varphi_0 = (\lambda B)^3 - 6(\lambda B) - 6R_q \eta(x_1)/(\lambda B)^2(\lambda B + 2)$, $\varphi_z = 3 - 2\varphi_0$, $R_q = q_1/q_z$, $\eta(x_1) = [1 - \varphi(x_1)]/\lambda(x_1)$, $\varphi(x) = e^{-\lambda x}(\cos \lambda x + \sin \lambda x)$, and $\xi(x) = e^{-\lambda x} \sin \lambda x$; k is the basic rigidity of the elastic coal sides in the roadway, $k = E_c/(1 - v_c^2)h_c$, and E_c, v_c, and h_c are the Young modulus, Poison ratio, and thickness of the coals, respectively; E is Young's modulus of the roadway roof; and I is the moment inertia of the roof beam.

Considering that the bending moment and deflection of each point in the cross section of the roadway are the same and equal to the bending moment and deflection at $x = -B/2$, Equations (3) and (4) can be generated:

$$M_r = \varphi_0 \frac{q_z B^2}{12} - \frac{3 q_z B^2}{8}, \tag{3}$$

$$y_r = \frac{1}{EI}\left\{\varphi_z \frac{q_z B^4}{192} + \frac{EI}{k}\left[q_z \lambda B + \varphi_0 \frac{q_z \lambda^2 B^2}{6}\right] \cdot + \frac{q_1}{\lambda x_1}[\lambda x_1 - \xi(x_1)] - \frac{q_z}{24}\left[\frac{B}{2}\right]^4\right\}, \tag{4}$$

where b and h are the width and thickness of the roof beam, respectively; q_s is the support strength from the hydraulic support; and q_a is the bearing capacity of roadway under the condition of bolt-mesh-anchor support. The maximum normal stress, that is, the maximum tension strength in the cross section of the roof bar is

$$\sigma_{max} = \frac{M_r y}{I} = \frac{6M_r}{bh^2} = \frac{(2\varphi_0 - 9)(q_z - q_s - q_a)B^2}{4bh^2}. \tag{5}$$

From Equations (4) and (5), it can be seen that deflection and the bending moment were caused by the upper load q_z in the roadway roof. Deflection results from the bending deformation causing the roof to settle and can be calculated by Equation (4). The bending moment causes the normal tension within the cross section of the roof bar and contributes to the fractures of the roof. The failure pattern of the roadway roof is assumed to be tension failure, and the critical condition of the roof to fracture under the support is when the maximum tension σ_{max} is equal to the ultimate tension strength $[\sigma]$ of the roadway roof as shown by

$$\sigma_{max} = \frac{(2\varphi_0 - 9)(q_z - q_s - q_a)B^2}{4bh^2} = [\sigma]. \tag{6}$$

The critical support strength of the hydraulic support is given by

$$q_s = q_z - q_a - \frac{4bh^2[\sigma]}{(2\varphi_0 - 9)B^2}. \tag{7}$$

To ensure stability of the surrounding rock, the hydraulic support must have a certain length of movable column,

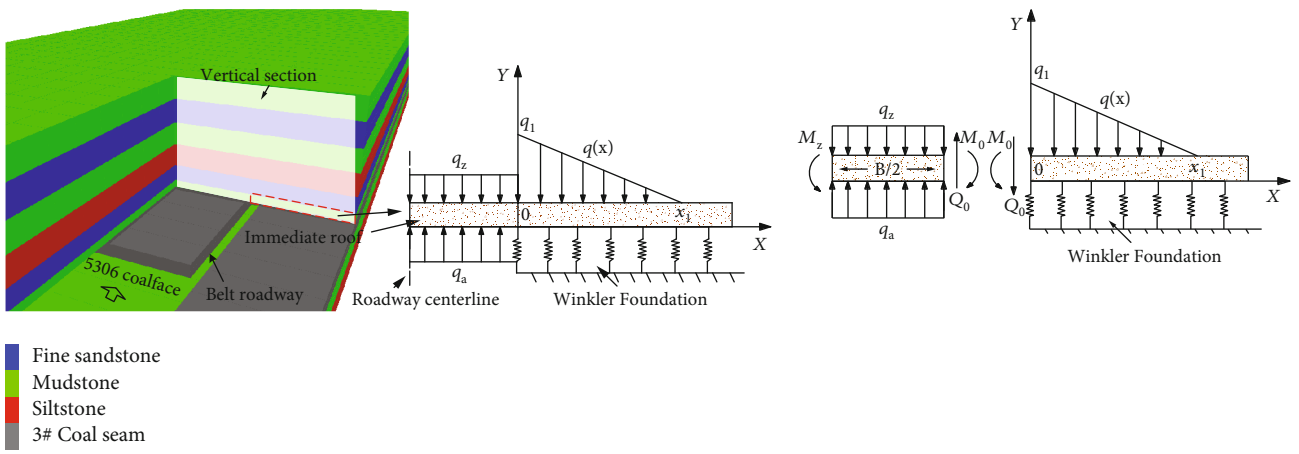

Figure 7: Cantilever beam model based on the Winkler foundation in the roadway roof: (a) mechanical model of the roadway roof; (b) analysis of the forces acting on the model.

which equals the settlement of the roof. According to Equation (4), the length of the movable column L should satisfy

$$L = y_r = \frac{1}{EI}\left\{\varphi_z \frac{q_z B^4}{192} + \frac{EI}{k}\left[q_z \lambda B + \varphi_0 \frac{q_z \lambda^2 B^2}{6}\right] \cdot + \frac{q_1}{\lambda x_1}\left[\lambda x_1 - \xi(x_1)\right] - \frac{q_z}{24}\left[\frac{B}{2}\right]^4\right\}. \quad (8)$$

4.1.3. Determination of the Roadway Support Parameters. The support strength and movable columns of the hydraulic supports in the roadway subjected to the front abutment pressure of the belt roadway in the 5306 coalface of the Tangkou coal mine were calculated from Equations (7) and (8). But the support distance from the coalface and the roof load q_z was the premise.

(1) Distribution of the Front Abutment Pressure. Based on the 3DEC model of the surrounding rock used in the analysis of roadway deformation, in the retreat direction, 36 measuring lines were placed in the middle of the belt roadway in the vertical section upward from mudstone immediate roof to record the vertical stress during the mining process, as shown in Figure 8(a). The vertical spacing of monitoring lines was 1 m, and the monitoring length was 100 m in front of the coalface. The layout direction of the monitoring lines was along the belt roadway. The date from the monitoring line where the maximum vertical stress was located was selected to describe the front abutment pressure. The layout of measuring lines and distribution of the front abutment pressure are shown in Figure 8.

During the mining process, the front abutment pressure in Figure 8(b) rapidly increased and then slowly decreased before it gradually became steady. The peak pressure, which was 43.73 MPa, occurred at a distance of 14.2 m in front of the coalface. The area with increased stress was in the range of 8.2–57.7 m in front of the coalface. Since the front abutment pressure in the stress-increased area usually causes the roof to settle and coal sides to contract, hydraulic support was applied in this area to ensure the safety of the roadway. Therefore, the support range of the belt roadway was kept at least 57.7 m from the 5306 coalface.

(2) Distribution of the Roadway Roof Load. Based on the above analysis, the roadway roof load q_z was monitored, and a unique measuring line was arranged between the mudstone immediate roof and fine sandstone main roof in the middle of the belt roadway. The vertical stress date measured by this measuring line was selected to describe the roadway roof load. The distributions of the roadway roof loads at 0 −57.7 m in front of the coalface are shown in Figure 9.

From Figure 9, it can be seen that the load q_z on the immediate roof also increased and then decreased before slowly becoming stable. The increase, decrease, and stabilization in the roadway roof load area occurred at 0–12.2 m, 12.2 −32.0 m, and 32.0–57.7 m in front of the coalface, respectively. The maximum roadway roof load, which was 0.164 MPa, was at 12.2 m in front of the coalface. At a distance of 32.0 m in front of the coalface, the roadway roof load became stable, with a constant value of 0.104 MPa. To simplify the expression of the roadway roof load distribution in the roadway, the loads at both ends of the coalface, the maximum roadway load, and the initial value when the roadway load area was stable were taken as characteristic values, and the linear fit of the loads when the load area increased, decreased, and stabilized was carried out. The roadway roof load q_z (unit: MPa) is shown in

$$q_z = \begin{cases} (0.54x + 9.87) \times 10^{-2} & (0 \le x \le 12.2), \\ -3 \times 10^{-3} x + 0.201 & (12.2 \le x \le 32.0), \\ 0.104 & (32.0 \le x \le 57.7). \end{cases} \quad (9)$$

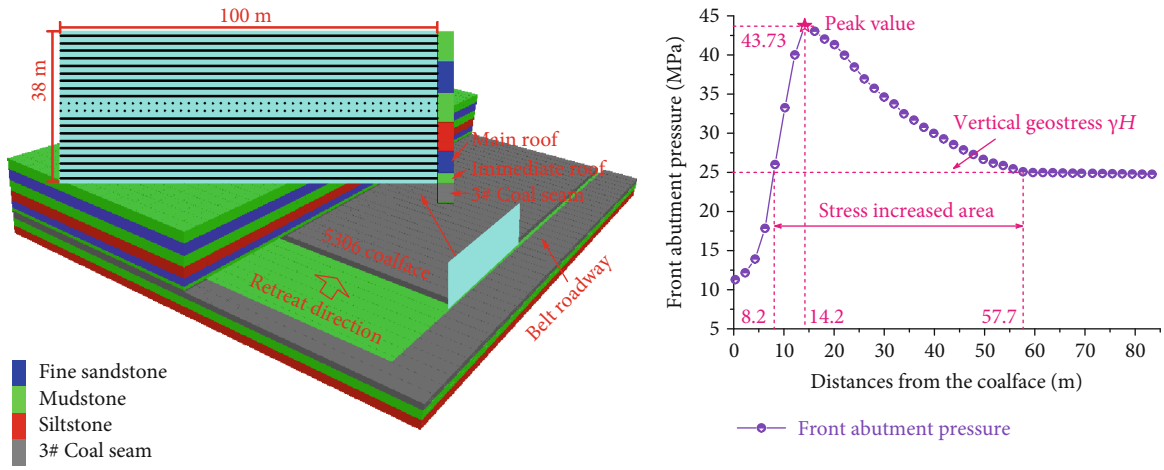

FIGURE 8: Layout of the measuring lines and distribution of the front abutment pressure: (a) measuring lines layout; (b) front abutment pressure distribution.

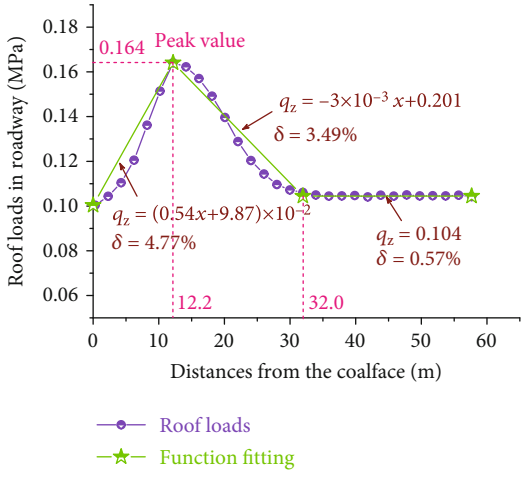

FIGURE 9: Distribution of the roof loads in roadway.

The average errors δ of the three values were 4.77%, 3.49%, and 0.57%, respectively, which were less than 5% or even 1%. This shows that Equation (9) can accurately describe the load distribution of the roadway roof.

(3) Calculation of the Roadway Support Parameters. Using the known roadway roof load q_z in combination with Equations (7) and (8), the support strength q_s and movable column length L of the hydraulic support in the roadway subjected to the front abutment pressure were calculated by inserting the parameters shown in Table 2.

The original design value for the support strength with bolt-mesh-anchor in the belt roadway of the coalface 5306 was 0.168 MPa, and the effective coefficient was 0.6. Thus, with the bolt-mesh-anchor support, the bearing capacity of the anchored surrounding rock itself q_a was 0.101 MPa. Based on the parameters in Table 2, the support strength q_s and movable column length L, as shown in Figure 10(a), were calculated. Additionally, based on the original support pattern and parameters in the roadway subjected to the front abutment pressure of belt roadway in the coalface 5306, as well as the support setting load that was taken as 60% of the support strength [18], the setting loads at different distances from the coalface are shown in Figure 10(b).

From Figure 10(a), it can be seen that the support strengths and movable column lengths of the supports at different locations exhibited the same trend, which consisted of three stages. In the ranges of 0–12.2 m, 12.2–32.0 m, and 32.0–57.7 m, both parameters increased linearly, decreased linearly, and became stable, respectively, as the distance from the coalface increased. The maximum support strength needed for the supports was 0.083 MPa, and the maximum movable column length was 280.3 mm, both occurring at a distance of 12.2 m in front of the coalface.

Figure 10(b) shows that the changing trend in the support setting load at different locations was consistent with that in the support strength and movable column length. As the distance from the coalface increased, the setting load of the hydraulic supports increased and subsequently decreased linearly, and the maximum setting load was 21.67 MPa at 12.2 m away from the coalface. When the distance of the advanced roadway was greater than 32.0 m away from the coalface, the setting load of single props became constant at 12.44 MPa.

In Figure 10(a), at 20 m in front of the 5306 coalface, the theoretical setting load and movable column length of the hydraulic supports were 14.97 MPa and 240.1 mm, respectively. At a distance of 35 m in front of the 5306 coalface, the theoretical setting load and movable column length of the single props were 12.44 MPa and 177.1 mm, respectively. However, the setting load and movable column length of the hydraulic supports in the field were 6.5 MPa (43.4% of the theoretical value) and 350 mm (56.5% of the theoretical value), respectively. Thus, at 20 m in front of the 5306 coalface, the setting load of the hydraulic supports in the field was too small, while the movable column length was too

Table 2: Basic parameters.

Parameter	Value	Parameter	Value	Parameter	Value
Depth of coal seam, H	992.8 m	Young's modulus of the coal seam, E_c	0.53 GPa	Thickness of immediate roof, h	2.5 m
Unit weight of overburden, γ	0.025 MN/m^3	Poisson's ratio of the coal seam, ν_c	0.37	Range of side abutment pressure, x_1	12.5 m
Thickness of coal seam, h_c	5.0 m	Span of the roadway, B	5.0 m	Peak value of front abutment pressure, q_1	25 MPa

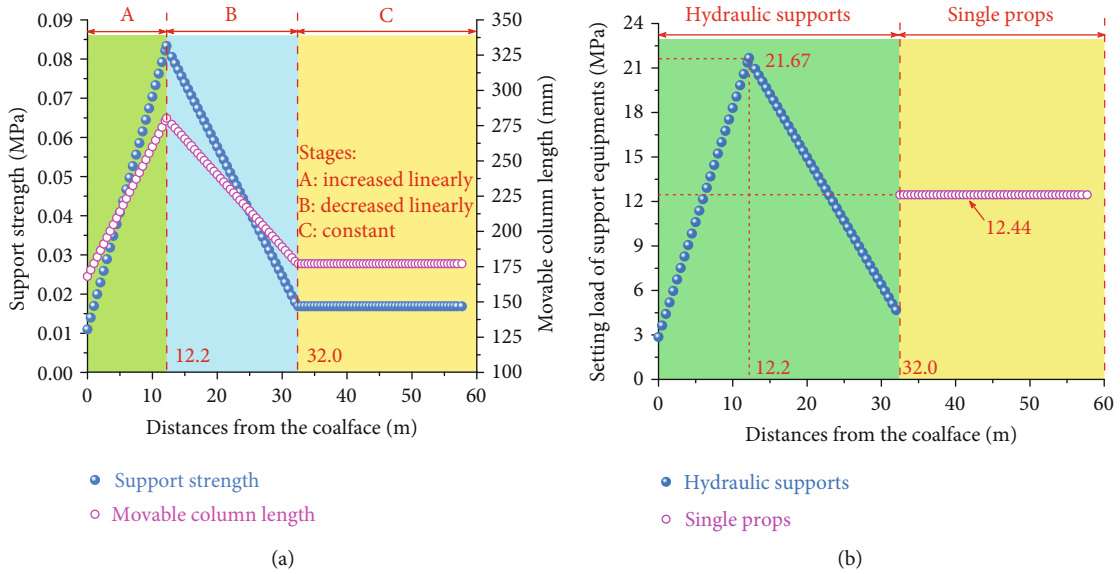

Figure 10: Support parameters in roadway of the 5306 coalface: (a) support strength and roof settlement; (b) setting load of supports.

large. However, at 35 m in front of the 5306 coalface, the movable column length of the single props in the field was significantly small. These results prove the accuracy of the explanation of roadway deformation and failure in Section 2.2.

4.2. Control Mechanism of Roadway Roof. In order to obtain the longtime stability control mechanism of roadway roof subjected to front abutment pressure, the same 3DEC numerical model was used to analyze the influence of different support strengths and movable column lengths of the supports. Since the working resistance of the hydraulic supports is the passive load from the roadway roof, the setting load is considered more practical in the coal mining. Therefore, the control effect of roadway under different conditions of support setting load and movable column length was analyzed.

4.2.1. Simulation Schemes. The roadway support of the belt roadway at 20 m in front of the coalface 5306 was selected as a baseline scheme for analysis, where the setting load and movable column length of the hydraulic support were 14.97 MPa and 240.1 mm, respectively. Another two schemes 0.6 and 1.4 times larger than their counterpart in the baseline group were added as a test and used in the analyses of the roadway deformation under different conditions of support setting load and movable column length. The schemes are summarized in Table 3.

4.2.2. Simulation Results. The numerical model established in this section is the same as that in Section 3.1. In order to realize and limit the movable characteristic of the hydraulic support in the numerical model, the method of limiting the maximum allowable vertical displacement of the hydraulic support was used to set the movable column length. In the process of the increase in the pressure on the hydraulic support from setting load to working resistance, the vertical displacement of the hydraulic support was set from 0 to the maximum allowable value linearly. Here, the maximum allowable value of vertical displacement of hydraulic support was its movable column length. The deformation of the surrounding rock in the different schemes is shown in Figure 11.

The deformation of the surrounding rock in scheme 1 was the smallest (Figures 11(a) and 11(b)), where the roadway had a settlement of 132.54 mm, a maximum vertical stress of 32.14 MPa, and a stress concentration coefficient of 1.29. Besides, the coal sides were well controlled, and no separation was found in the roof. In scheme 2 (where the movable column length was the same and the setting load was reduced by 0.6 times the theoretical value), the roadway deformation was higher than that in scheme 1, the roof separation occurred between the immediate roof and main roof,

Table 3: Schemes of numerical simulations.

No.	Setting load (MPa)	Movable column length (mm)	Note
Scheme 1	14.97	240.1	(1) Scheme 1 was the baseline scheme. (2) The aim of schemes 1, 2, and 3 was to study the effect of the setting load. (3) The aim of schemes 1, 4, and 5 was to study the effect of the movable column length.
Scheme 2	8.98	240.1	
Scheme 3	20.96	240.1	
Scheme 4	14.97	144.1	
Scheme 5	14.97	336.1	

and vertical stress developed in a deeper area in the coal sides (Figures 11(c) and 11(d)). The roadway roof had a settlement of 384.68 mm and a peak vertical stress of 44.33 MPa. In scheme 3 (where the movable column length was the same and the setting load was reduced to 1.4 times the theoretical value), the value of deformation was between those obtained in schemes 1 and 2 (Figures 11(e) and 11(f)), where the roadway roof had a settlement of 334.56 mm and a maximum vertical stress of 38.44 MPa. In scheme 4 (where the setting load was the same and the movable column length was reduced by 0.6 times the theoretical value), the deformation of the surrounding rock was very serious. The roof separation became more evident and formed a net trough, the contraction deformation of the coal sides was large, and an area of increased stress was found, where the props and the immediate roof met (Figures 11(g) and 11(h)). The roadway roof had a settlement of 406.40 mm and a maximum vertical stress of 45.56 MPa. In scheme 5 (where the setting load was the same and the movable column length was reduced by 1.4 times the theoretical value), the deformation of the surrounding rock was the largest; the roof separation became more evident than that in scheme 4, the coal sides formed an arc shape, and the bolts in the coal sides and roof moved to different extents (Figures 11(i) and 11(j)). The roadway roof had a settlement of 506.56 mm and a maximum vertical stress of 48.09 MPa, which were 3.82 and 1.50 times larger than their counterparts in scheme 1, respectively. The values of the different parameters in the different schemes are shown in Table 4.

4.2.3. Coupling Mechanism of Supports and Anchored Surrounding Rock. The roadway deformation subjected to the front abutment pressure in scheme 1 fell within an allowable range and the surrounding rock control was satisfactory. Excessively large or small setting loads and movable column lengths of the hydraulic supports or single props caused a large deformation in the roadway, resulting in roof separation and significant settlement, large contraction of the coal sides, roof falling, and concentrated stresses in the surrounding rock. Therefore, coupling mechanisms of strength and deformation of the supports and anchored surrounding rock were analyzed based on the deformation characteristics of the roadway in the field and numerical models.

(1) Strength Coupling. From to the above results, it was found that the roadway roof load was influenced by the front abutment pressure. Most of the roof load was borne by the anchored surrounding rock when the support setting load was too small and sufficient support could not be provided in time. If the sum of the anchoring strength of the surrounding rock and the support setting load was still less than the roadway roof load, the failure occurred as a result of large settlements, roof separation, or roof falling. In the meantime, the roof load transferred to the surrounding rock and caused an extrusion and stress concentration in the coal sides. The deformation and failure of the roadway also induced a decreased bearing capacity and an anchoring strength of the surrounding rock, causing a further roadway deformation (Figures 11(c) and 11(d)). Both the field monitoring data for the roadway deformation at 20 m away from the coalface and the results of scheme 2 validate the analysis. Conversely, if the support setting load was too large, the anchored surrounding rock exhibits some deformation when the hydraulic supports were installed, leading to a decrease in the anchoring strength of the surrounding rock and thus a failure to fully develop the bearing capacity of the anchored surrounding rock (Figures 11(e) and 11(f)). The roadway roof load was mainly borne by the supports, which increased the energy consumption and the possibility of support crush.

(2) Deformation Coupling. An excessively small movable column length of the hydraulic supports meant that the retraction was less than the roadway roof settlement. Thus, the roof retraction in the early stages of the roadway deformation was compatible with the roof settlement. When the roof retraction reached its maximum allowable value, the hydraulic supports did not retract anymore. Further roof settlement caused the hydraulic supports to penetrate the floor or the roadway roof (Figure 3(c)), leading to a failure of the anchored surrounding rock and a subsequent strength reduction in the anchored surrounding rock and an increase in the support load. Moreover, a too small hydraulic support retraction caused a stress concentration, where the hydraulic support and the roadway roof met (Figures 6(b) and 11(h)). However, an

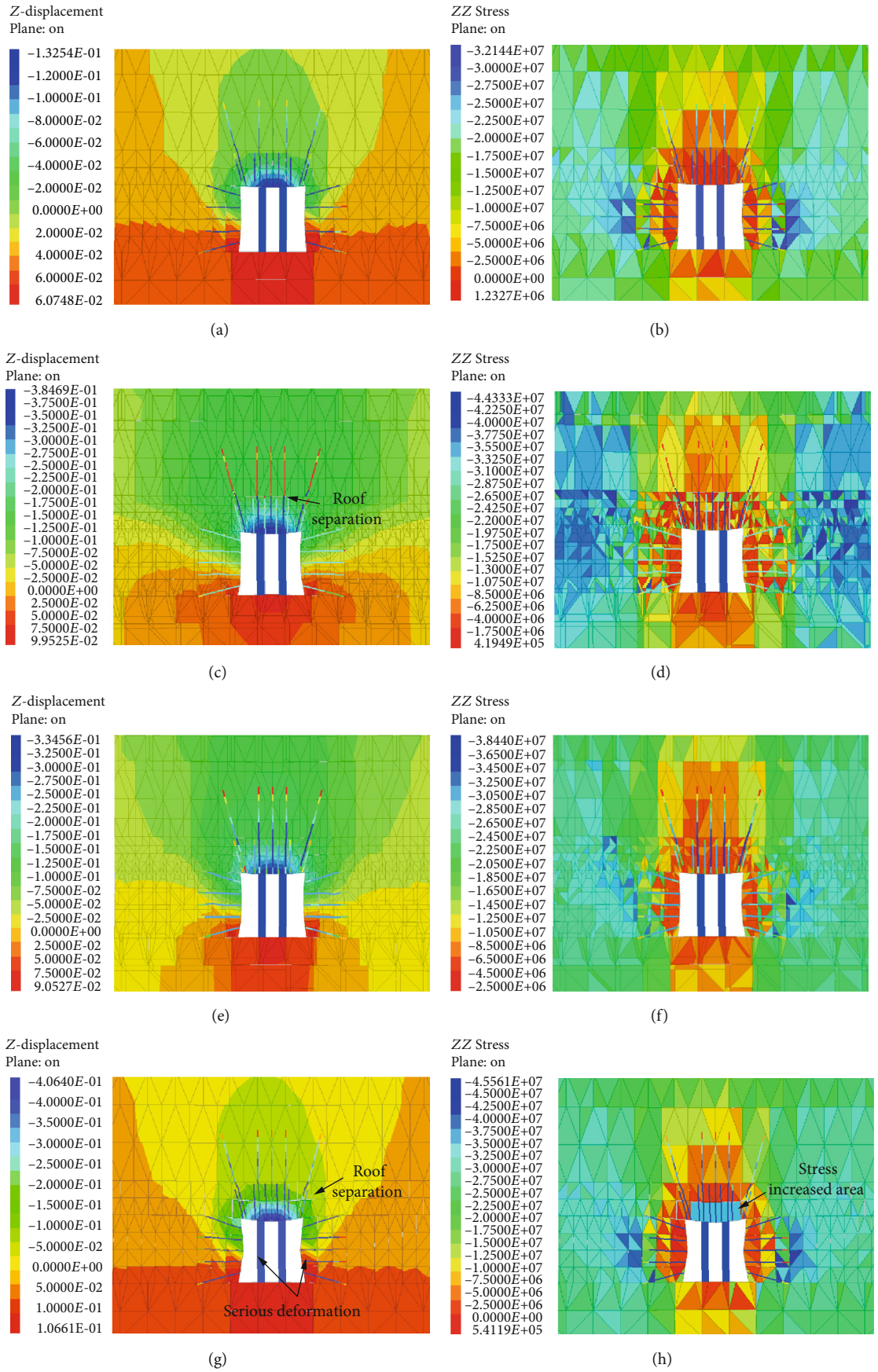

Figure 11: Continued.

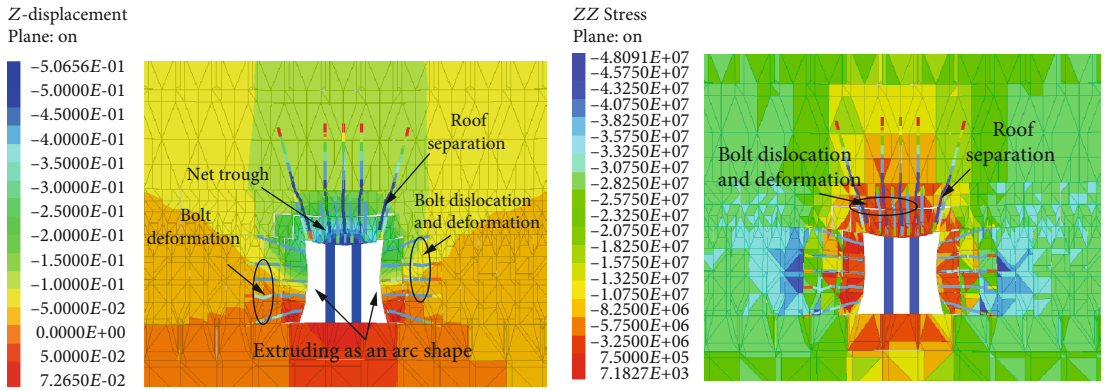

Figure 11: Numerical simulation results of surrounding rock deformation in the different schemes: (a) cloud graph of vertical displacement of scheme 1; (b) cloud graph of vertical stress of scheme 1; (c) cloud graph of vertical displacement of scheme 2; (d) cloud graph of vertical stress of scheme 2; (e) cloud graph of vertical displacement of scheme 3; (f) cloud graph of vertical stress of scheme 3; (g) cloud graph of vertical displacement of scheme 4; (h) cloud graph of vertical stress of scheme 4; (i) cloud graph of vertical displacement of scheme 5; (j) cloud graph of vertical stress of scheme 5.

Table 4: Roadway deformation in the different schemes.

No.	Roof convergence (mm)		Maximum vertical stress (MPa)		Stress concentration coefficient
	Simulated value	The ratio of the value to scheme 1	Simulated value	The ratio of the value to scheme 1	
Scheme 1	132.54	1.00	32.14	1.00	1.29
Scheme 2	384.68	2.90	44.33	1.38	1.77
Scheme 3	334.56	2.52	38.44	1.20	1.54
Scheme 4	406.40	3.07	45.56	1.42	1.82
Scheme 5	506.56	3.82	48.09	1.50	1.92

excessively large hydraulic support movable column length meant that the retraction of the hydraulic support was larger than the roof settlement; thus, the hydraulic supports settled along with the roof. When the roof settlement reached its maximum value, the hydraulic supports still had margin for retraction, leading to a failure of the hydraulic supports that achieved the design work resistance, a lack of support strength, and a large amount of load transferred to the anchored surrounding rock. However, due to the limited bearing capacity of the anchored surrounding rock, an excessive roadway roof load would induce roof separation, roof falling, extrusion of coal sides, and dislocation deformation of the anchors (Figures 11(i) and 11(g)), finally causing a decrease in the strength in the anchored surrounding rock and serious failure.

4.3. Optimization of Support Parameters. Based on analysis of the relation between the hydraulic support and the anchored surrounding rock, theoretical values were set for the setting load and movable column length (Figure 10) in the roadway subjected to the front abutment pressure of the belt roadway in the coalface 5306 of the Tangkou coal mine. The displacements between the roof and floor and between the coal sides, in addition to roof separation, were recorded. Three groups of hydraulic support were applied at 0–32 m in front of the coalface (model: ZQL2×2500/23/42W), and single props were applied at 32–60 m in front of the coalface (model: DW45-250/110XL(G)), along with an articulated roof beam (model: DJB-800): a "one beam per prop" pattern was employed. Based on the calculated results shown in Figure 10, the support setting loads q_i (units: MPa) at different positions of the roadway satisfied

$$q_i = \begin{cases} 1.542x + 2.860 & (0 \le x \le 12.2), \\ -0.858x + 32.128 & (12.2 \le x \le 32.0), \\ 12.443 & (32.0 \le x \le 60.0). \end{cases} \quad (10)$$

The movable column length L_i (units: mm) of the supports at different positions in the roadway satisfied

$$L_i = \begin{cases} 9.196x + 168.083 & (0 \le x \le 12.2), \\ -5.124x + 342.780 & (12.2 \le x \le 32.0), \\ 177.109 & (32.0 \le x \le 60.0). \end{cases} \quad (11)$$

5. Field Observation

When the retreat length was 650 m from the open-off cut, the field observation was carried out within 100 m in front of the coalface to verify the reliability of the optimized support parameters. The layout of the stations monitoring the displacements between the roof and floor and between the coal sides is shown in Figure 12. Two roof separation stations were placed at 50 m and 100 m in front of the coalface. The deep and shallow base points of the roof separation stations were in the middle of the fine sandstone main roof and mudstone immediate roof. The surface deformation of the advanced roadway and the amount of roof separation are shown in Figure 13.

By using the optimized parameters of the roadway supports, the roadway deformation showed an evident decrease in its value. The ultimate displacements between the roof and floor were 275.5–300.8 mm, with an average value of 287.0 mm. The ultimate displacements between the coal sides were 209.6–233.2 mm, with an average value of 220.8 mm. The maximum amount of roof separation was approximately 45 mm, and the integrity of the surrounding rock was good. The roadway deformation subjected to front abutment pressure was within an allowable range and did not influence the mining process. Additionally, the integrity of the roadway roof in the surrounding rock at 20 m and 35 m in front of the coalface was well maintained, and no large roof separation or net trough was found (Figure 14). The displacements between the coal sides were small, and the extrusion became significantly less. The results show that when the setting loading q_i of the hydraulic supports and movable column length L_i satisfied Equations (10) and (11), the hydraulic support and anchored surrounding rock coupling was achieved, where the bearing capacity of the anchored surrounding rock was fully developed. At this point, the roadway deformation was effectively controlled, and the control effect of the surrounding rock in the roadway subjected to front abutment pressure was greatly improved.

6. Discussion and Conclusion

During underground coal mining at 1000 m depth, with an increased crustal stress and the front abutment pressure, the integrity of the surrounding rock was difficult to control. Roadway deformation and failure, such as roadway roof fracture, roof falling, settlement, roof separation, and extrusion of coal sides, were likely to occur, when inappropriate roadway support parameters were used in the roadway subjected to front abutment pressure, thereby seriously influencing the coal mining and the safety of miners. Based on the mechanism analysis of the roadway deformation and failure, it was found that the surrounding rock failure was closely related to the support load and movable column length of supports (hydraulic supports and single props).

Based on the Winkler foundation assumption, an improved mechanical model of the roadway roof subjected to the front abutment pressure was established considering the supporting effect of the supports (hydraulic supports and single props) on roof. According to the mechanical model, the mathematical expressions of the support strength and movable column length of the supports were deducted (Equations (7) and (8)). Furthermore, the optimized supporting parameters of the supports in the belt roadway of the 5306 coalface of the Tangkou coal mine were obtained. The results show that under the front abutment pressure, the setting load and movable column length of supports increased and then decreased before slowly becoming stable. The support range of roadway was at least 60 m from the coalface. At the same time, the maximum setting load and movable column length of hydraulic supports were 21.67 MPa and 280.3 mm, respectively, at 12.2 m away from the coalface. When the distance of the belt roadway was greater than 32.0 m away from the coalface, the setting load and movable column length of single props became constant at 12.44 MPa and 177.1 mm, respectively.

Different from that in other locations, the stability control mechanism of roadway subjected to the front abutment pressure showed that the longtime effective support of roadway roof required the strength and the deformation coupling of the supports (hydraulic supports or single props) and the anchored surrounding rock (bolt-cable support). Appropriate support strength of the supports and a fully developed bearing capacity of anchored surrounding rock were required to achieve the strength coupling; a compatible movable column length of the supports with the roadway roof settlement was required to achieve the deformation coupling. Excessively large support strength or small movable column length of supports caused the deformation and failure of roadway roof, decreased in the anchoring strength of the surrounding rock, and even led to the roof falling disaster which poses threats to the life of miners. On the contrary, the small support strength or large movable column length of support induced a roof separation, extrusion of coal sides, and dislocation deformation of the anchors. A high or low value other than the optimum value affected the occurrence rate of roof falling disaster that can adversely affect the safety of miners.

Field tests show that, by applying the optimized support strength and movable column length of support to the belt roadway of the 5306 coalface of the Tangkou coal mine, the roadway deformation was small, the extrusion and roof separation became significantly less, the roof falling disaster did not occur, the stability control of the roadway subjected to front abutment pressure, and the disaster control of roof falling was realized. Moreover, the safety of miners was guaranteed by applying the optimized support strength and movable column length of support to the belt roadway of the 5306 coalface of the Tangkou coal mine.

As the plastic zone in the surrounding rock of roadway was not considered in the mechanical model established in Section 4.1, the theoretical value of roadway deformation will

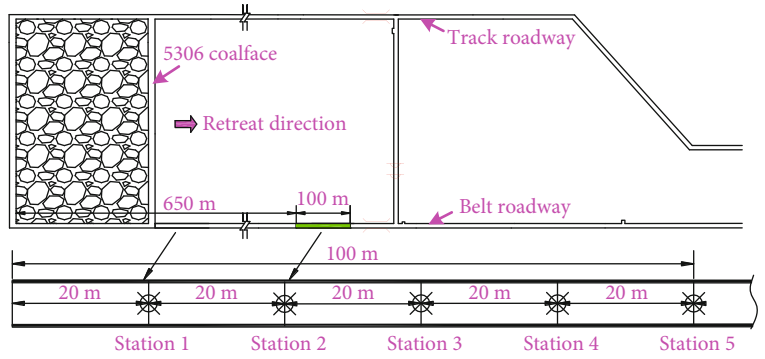

Figure 12: Layout of the roadway deformation monitoring stations.

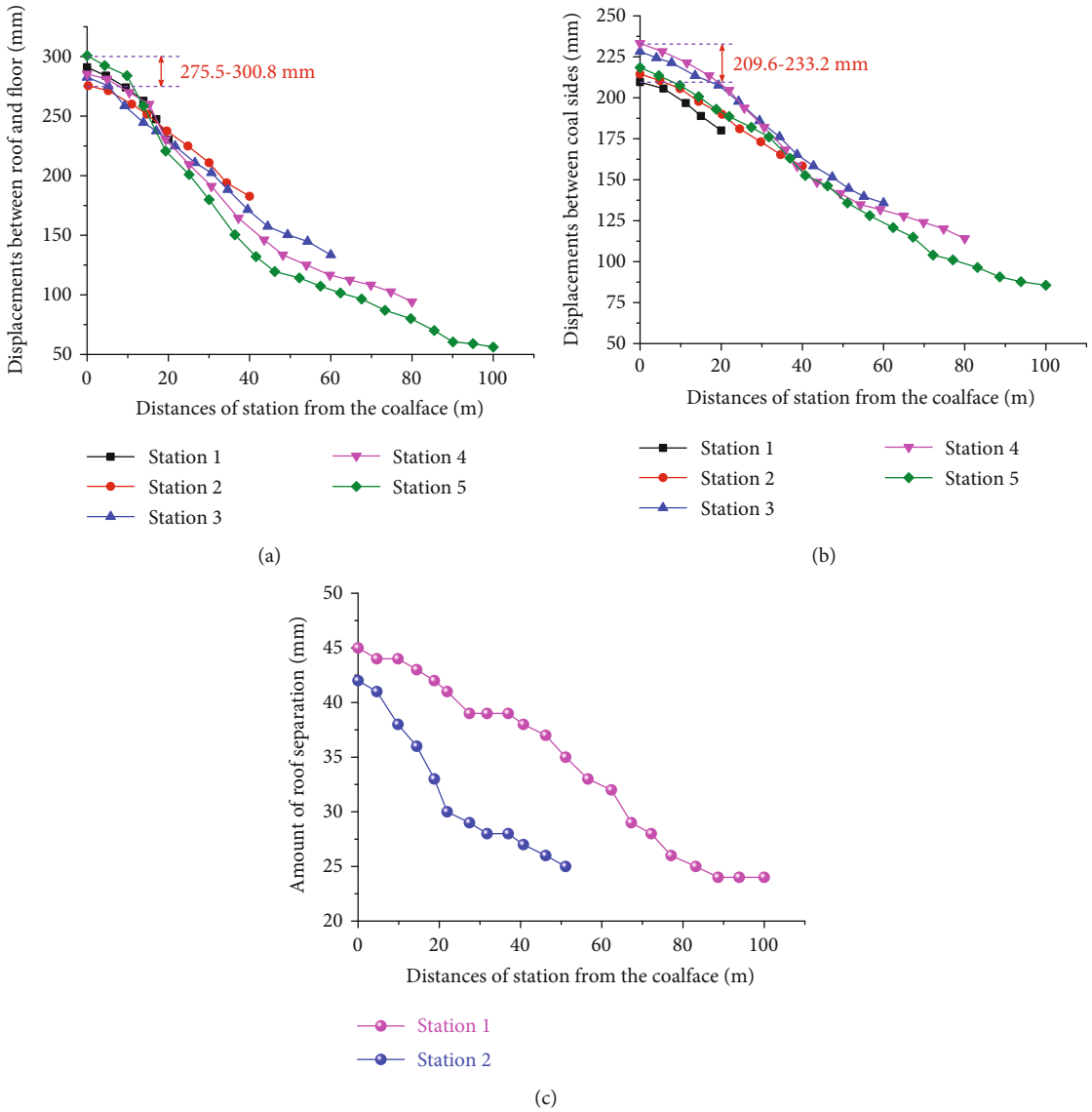

Figure 13: Surface deformation and amount of roof separation in the roadway: (a) displacement between the roof and floor; (b) displacement between the coal sides; (c) amount of roof separation.

(a) (b)

Figure 14: Roadway support with optimized parameters: (a) 20 m in front of the workface; (b) 35 m in front of the workface.

be less than the actual value. However, the practice shows that the error of roadway deformation caused by the mechanical model does not affect the use of roadway on-site. In order to eliminate the error of roadway deformation between the theory and the practice, the mechanical model in this paper should be further improved in the future research considering the plastic deformation of roadway surrounding.

Data Availability

The data used to support the findings of this study are included within the article. The detailed research data for Figures 8–10 can be found in "Supplementary Materials" of the present paper.

Conflicts of Interest

The authors declare that they have no conflicts of interest.

Acknowledgments

This work was financially supported by the National Natural Science Foundation of China (grant numbers 51774268, 51974291) and the Independent Research Project of State Key Laboratory of Coal Resources and Safe Mining, CUMT (grant number SKLCRSM18X007). The authors are grateful to the Tangkou coal mine in Shandong for the supports of surface deformation and amount of roof separation in the belt roadway of workface 5306 on-site.

Supplementary Materials

The supplementary materials of the present paper include the detailed research data of Figures 8–10, which are available to readers. *(Supplementary Materials)*

References

[1] D. Zhu, Y. Wu, Z. Liu, X. Dong, and J. Yu, "Failure mechanism and safety control strategy for laminated roof of wide-span roadway," *Engineering Failure Analysis*, vol. 111, article 104489, 2020.

[2] L. J. Zhou, Q. G. Cao, K. Yu, L. L. Wang, and H. B. Wang, "Research on occupational safety, health management and risk control technology in coal mines," *International Journal of Environmental Research and Public Health*, vol. 15, no. 5, p. 868, 2018.

[3] F. Gao, D. Stead, and H. Kang, "Numerical simulation of squeezing failure in a coal mine roadway due to mining-induced stresses," *Rock Mechanics and Rock Engineering*, vol. 48, no. 4, pp. 1635–1645, 2015.

[4] C. Wang, Y. Wang, and S. Lu, "Deformational behaviour of roadways in soft rocks in underground coal mines and principles for stability control," *International Journal of Rock Mechanics and Mining Sciences*, vol. 37, no. 6, pp. 937–946, 2000.

[5] M. R. Islam and R. Shinjo, "Mining-induced fault reactivation associated with the main conveyor belt roadway and safety of the Barapukuria coal mine in Bangladesh: constraints from BEM simulations," *International Journal of Coal Geology*, vol. 79, no. 4, pp. 115–130, 2009.

[6] G. Wang and Y. Niu, "Study on advance hydraulic powered support and surrounding rock coupling support system and suitability," *Coal Science and Technology*, vol. 44, pp. 19–25, 2016.

[7] G. S. P. Singh and U. K. Singh, "A numerical modeling approach for assessment of progressive caving of strata and performance of hydraulic powered support in longwall workings," *Computers and Geotechnics*, vol. 36, no. 7, pp. 1142–1156, 2009.

[8] R. Trueman, G. Lyman, and A. Cocker, "Longwall roof control through a fundamental understanding of shield-strata interaction," *International Journal of Rock Mechanics and Mining Sciences*, vol. 46, no. 2, pp. 371–380, 2009.

[9] A. K. Verma and D. Deb, "Numerical analysis of an interaction between hydraulic-powered support and surrounding rock strata," *International Journal of Geomechanics*, vol. 13, no. 2, pp. 181–192, 2013.

[10] A. Mangal and P. S. Paul, "Rock mechanical investigation of strata loading characteristics to assess caving and requirement of support resistance in a mechanized powered support longwall face," *International Journal of Mining Science and Technology*, vol. 26, no. 6, pp. 1081–1087, 2016.

[11] Y. Ma and S. Zhong, "Study on the relationship between hydraulic support on the working face with large mining

height and surrounding rock," *Advances in Materials Research*, vol. 328-330, pp. 1671–1674, 2011.

[12] Y. Yuan, S. Tu, X. Zhang, and B. Li, "System dynamics model of the support-surrounding rock system in fully mechanized mining with large mining height face and its application," *International Journal of Mining Science and Technology*, vol. 23, no. 6, pp. 879–884, 2013.

[13] S. S. Peng, "Support capacity and roof behaviour at longwall faces with shield supports," *International Journal of Mining and Geological Engineering*, vol. 5, no. 1, pp. 29–57, 1987.

[14] J. X. Yang, C. Y. Liu, and B. Yu, "The interaction between face support and surrounding rock and its rib weakening mechanism in hard coal seam," *Acta Montanistica Slovaca*, vol. 1, 2017.

[15] R. Trueman, G. Lyman, M. Callan, and B. Robertson, "Assessing longwall support-roof interaction from shield leg pressure data," *Mining Technology*, vol. 114, no. 3, pp. 176–184, 2013.

[16] S. Budirský, "Interaction of powered supports and the strata in coal seams under a heavy roof," *International Journal of Mining Engineering*, vol. 3, no. 2, pp. 113–138, 1985.

[17] G. S. P. Singh and U. K. Singh, "Numerical modelling based assessment of setting load requirement for optimum performance of powered roof supports in longwall workings," *Mining Technology*, vol. 118, no. 2, pp. 109–114, 2013.

[18] G. S. P. Singh and U. K. Singh, "Prediction of caving behavior of strata and optimum rating of hydraulic powered support for longwall workings," *International Journal of Rock Mechanics and Mining Sciences*, vol. 47, no. 1, pp. 1–16, 2010.

[19] G. Xu and Z. Liu, "The interaction relationship between support setting load and surrounding rock," *Advances in Materials Research*, vol. 962-965, pp. 344–351, 2014.

[20] D. Bakun-mazor, Y. H. Hatzor, and W. S. Dershowitz, "Modeling mechanical layering effects on stability of underground openings in jointed sedimentary rocks," *International Journal of Rock Mechanics and Mining Sciences*, vol. 46, no. 2, pp. 262–271, 2009.

[21] Q. Zhang, H. Jia, L. Fan, X. Zhao, Z. Wang, and J. Xing, "The detection research of roadway roof strata structure in coal seam," *Advances in Materials Research*, vol. 734-737, pp. 677–681, 2013.

[22] X. Shengrong, G. Mingming, C. Dongdong et al., "Stability influence factors analysis and construction of a deep beam anchorage structure in roadway roof," *International Journal of Mining Science and Technology*, vol. 28, no. 3, pp. 445–451, 2018.

[23] B. K. Hebblewhite and T. Lu, "Geomechanical behaviour of laminated, weak coal mine roof strata and the implications for a ground reinforcement strategy," *International Journal of Rock Mechanics and Mining Sciences*, vol. 41, no. 1, pp. 147–157, 2004.

[24] A. Sofianos, "Analysis and design of an underground hard rock voussoir beam roof," *International Journal of Rock Mechanics and Mining Sciences & Geomechanics Abstracts*, vol. 33, no. 2, pp. 153–166, 1996.

[25] F. Chase, C. Mark, and K. Heasley, "Deep cover pillar extraction in the US coalfields," in *21st International conference on ground control in mining*, pp. 68–75, Morgantown, 2002.

[26] I. Canbulat, "Improved roadway roof support design for Anglo American Metallurgical Coal's underground operations," *Mining Technology*, vol. 120, no. 1, pp. 1–13, 2013.

[27] S. C. Tadolini, P. W. Kraus, and A. Worbois, "High capacity tensioned cable bolts for tailgates support," in *19th International conference on ground control in mining*, pp. 59–66, Morgantown, 2000.

[28] B. Shen, "Coal mine roadway stability in soft rock: a case study," *Rock Mechanics and Rock Engineering*, vol. 47, no. 6, pp. 2225–2238, 2014.

[29] H. P. Kang, J. Lin, and M. J. Fan, "Investigation on support pattern of a coal mine roadway within soft rocks – a case study," *International Journal of Coal Geology*, vol. 140, pp. 31–40, 2015.

[30] C. Carranza-Torres, "Analytical and numerical study of the mechanics of rockbolt reinforcement around tunnels in rock masses," *Rock Mechanics and Rock Engineering*, vol. 42, no. 2, pp. 175–228, 2009.

[31] L. Jiang, H. S. Mitri, N. Ma, and X. Zhao, "Effect of foundation rigidity on stratified roadway roof stability in underground coal mines," *Arabian Journal of Geosciences*, vol. 9, no. 1, 2016.